HETEROCYCLES, Vol. 100, No. 9, 2020, pp. 1463 - 1472. © 2020 The Japan Institute of Heterocyclic Chemistry
Received, 1st June, 2020, Accepted, 6th July, 2020, Published online, 14th July, 2020
DOI: 10.3987/COM-20-14297

REACTIVITY OF THE ENAMINE TAUTOMER OF A CYCLIC 1,4-DIAZADIENE WITH A DIKETONE

Kazuhide Nakahara,[a*] Koki Yamaguchi,[b] and Hisao Kansui [c]

[a] Department of Integrative Pharmaceutical Sciences, Faculty of Pharmaceutical Sciences, Setsunan University, 45-1 Nagaotoge-cho, Hirakata, Osaka 573-0101, Japan; E-mail address; kazuhide.nakahara@pharm.setsunan.ac.jp [b] Laboratory of Molecular Design, Faculty of Pharmaceutical Sciences, Sojo University, 4-22-1 Ikeda, Nishi-ku, Kumamoto 860-0082, Japan [c] Laboratory of Organic Chemistry, Faculty of Pharmaceutical Sciences, Sojo University, 4-22-1 Ikeda, Nishi-ku, Kumamoto 860-0082, Japan

Abstract – Cyclic 1,4-diazadiene (2,3-dihydro-5-methyl-6-phenylpyrazine) and diketone (1-phenyl-1,2-propanedione) yielded two products *via* dehydration–condensation of the diamine and diketone moieties when a mixture of H_2O and MeOH was used as the solvent. The structures of the new products were established by 2D NMR analysis. Single-crystal X-ray structural characterization and density functional theory calculations allowed us to determine that this reaction took place *via* reaction of the enamine tautomer.

N-Heterocycles are widely present in bioactive organic compounds such as pharmaceuticals.[1] Among heterocyclic compounds, pyrazines, which can be isolated from foods,[2] exhibit various properties.[3] Dihydropyrazines (DHPs), which are pyrazine precursors for the Maillard reaction, can generate radicals[4] and have a high chemical reactivity.[5,6] Particularly, we are interested in the reactivity of cyclic 1,4-diazadienes as DHPs and have made them our research focus.

In a previous paper,[5] we reported the reaction between the lone pair on the nitrogen of cyclic 1,4-diazadienes and ketenes. Herein, we report that the enamine tautomer of a cyclic 1,4-diazadiene shows different reactivity from that previously reported. This change in reactivity is not unprecedented, as when the dimerization of DHPs occurs,[6] they tautomerize during the early stages of cyclization, resulting in an ene reaction between the -NH-C=C moiety of enamine-type DHPs and the C=N moiety of imine-type DHPs.

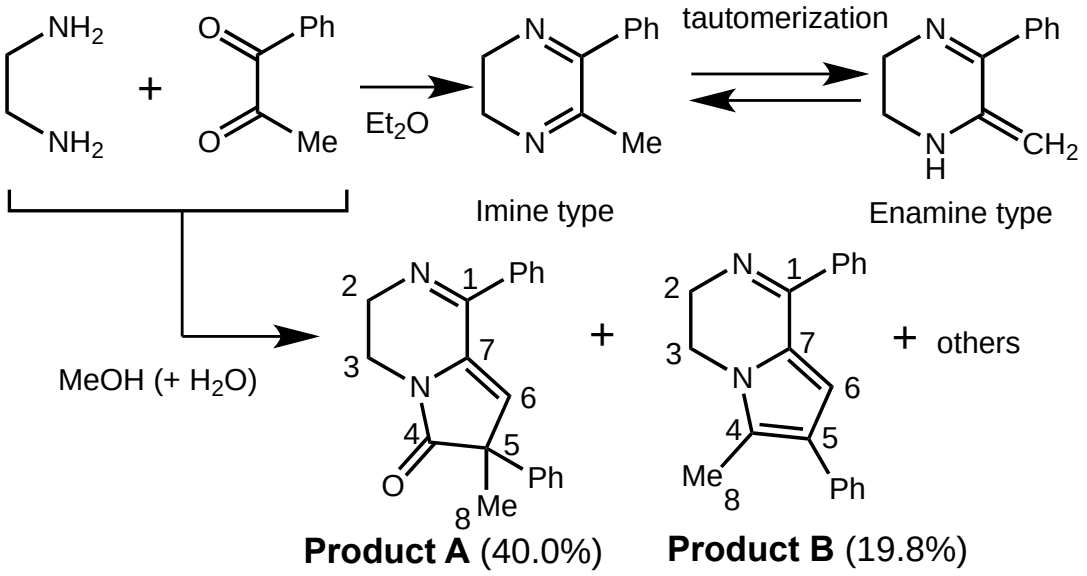

Figure 1. Reaction between the diamine and diketone

When forming a cyclic 1,4-diazadiene *via* dehydration–condensation of a diamine and diketone, **products A** and **B** were obtained when a mixture of MeOH and H_2O was used as the solvent due to subsequent reaction of the 1,4-diazadiene with the diketone (Figure 1). In the ^{1}H NMR spectrum of **product A**, methyl protons from C8 were observed at 1.72 ppm, methylene protons from C3 and C2 were observed at 3.68 and 4.07 ppm, respectively, and the methine proton from C6 was observed at 5.93 ppm. Moreover, the following functional groups were observed in the ^{13}C NMR spectrum: a methyl carbon at 23.7 ppm; methylene carbons at 35.7 and 49.2 ppm; a quaternary carbon at 54.8 ppm; alkene carbons at 111.7 and 120.2 ppm; phenolic carbons at 127.5, 128.4, 129.6, and 137.7 ppm; an imine carbon at 160.0 ppm; and a carbonyl carbon at 178.7 ppm. In the infrared spectrum, an absorption at 1447.3 cm^{-1} demonstrated the presence of an imine functional group, while an absorption at 1707.7 cm^{-1} was recognized as a ketone. Furthermore, a fragment peak was observed at *m/z* = 303.2 (M^{+}+1) in the mass spectrum. Overall, these findings demonstrate that **product A** had a γ-lactam ring. The ^{1}H and ^{13}C NMR peaks of **product B** are listed in Table 1 along with the data for **product A**. In order to confirm the assignments of the NMR spectra of **products A** and **B**, the correlations between the positions of the hydrogen and carbon atoms were examined by heteronuclear multiple bond correlation (HMBC) experiments (Table 1) using 2D NMR spectroscopy. To confirm the structure that was estimated from the spectral results, single-crystal X-ray analysis of **product A** was performed, and the resulting structure is shown in Figure 2.

In order to elucidate the mechanism of formation for **product A**, density functional theory (DFT) calculations were performed.[7] First, we considered pinacol rearrangement[8] based on pinacolone-like structural characteristics but did not fit the reaction conditions, which involved a room-temperature reaction using potassium hydroxide as a base for dehydration and MeOH as a reaction solvent. Next, we

proposed a mechanism that focuses on a nucleophilic reaction of the enamine, followed by cyclization and rearrangement (Figure 3).

Table 1. NMR data and HMBC relationships for **products A** and **B**

Position No. *	**Product A**			**Product B**		
	^{13}C NMR	^{1}H NMR	HMBC	^{13}C NMR	^{1}H NMR	HMBC
1	160.0			160.5		
2	49.2	4.07, 2H	1, 3	47.9	4.03, 2H	1, 3
3	35.7	3.68, 2H	2	39.2	3.93, 2H	2, 4
4	178.7			123.2		
5	54.8			123.7		
6	111.7	5.93, 1H	1, 4, 5	112.5	6.52, 1H	5, 7
7	120.2			125.9		
8	23.7	1.72, 3H	4, 5, 6, 7	10.6	2.46, 3H	4, 5

*Position No. relates to the structures shown in **Figure 1**.

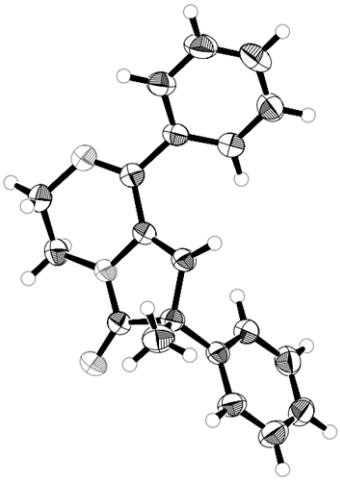

Figure 2. ORTEP diagram of **product A**

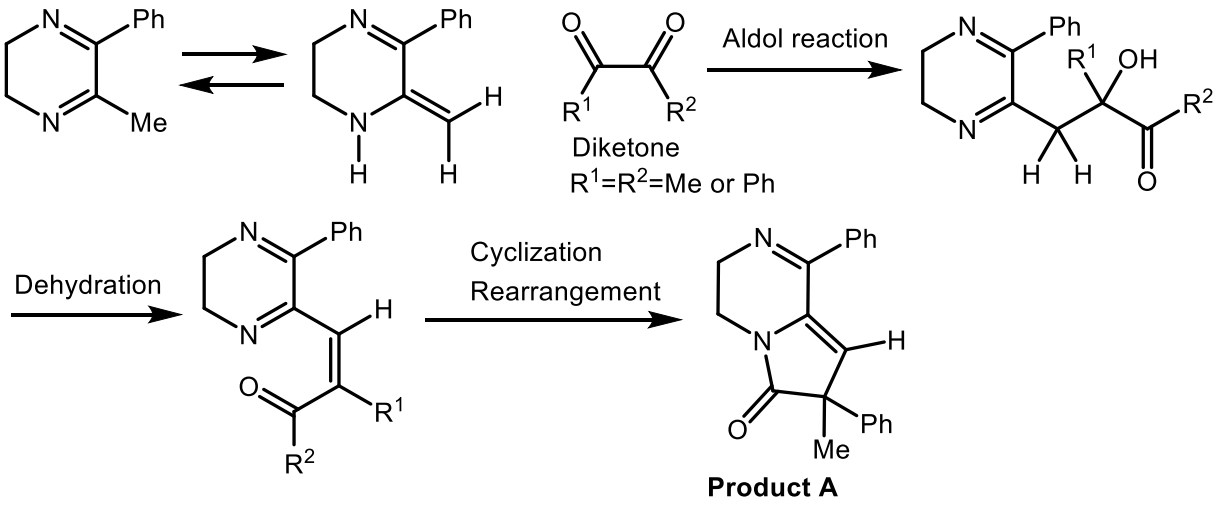

Figure 3. Proposed formation mechanism of **product A**

Previous studies have reported that imine–enamine tautomerization in cyclic 1,4-diazadienes has a high theoretical activation energy for intramolecular hydrogen transfer, but that this energy is much lower if hydrogen transfer takes place *via* H_2O.[9] Additionally, imine–enamine tautomerization in 1,2,3,5,6,7-hexahydroquinoxaline and 2,3,5,6,7,8-hexahydroquinoxaline has been reported to be solvent dependent, with highly polar solvents tending to increase the enamine (1,2,3,5,6,7-hexahydroquinoxaline) ratio.[10] As per these reports, this reaction was presumed to take place *via* the tautomerization of an imine to an enamine under the influence of a polar solvent, with enamine subsequently reacting with a diketone (Figure 4). The reaction of enamine with diketone was predicted to be a concerted reaction involving both C-C bond formation and proton transfer *via* a transition state (TS). The reaction was analogous to the aldol reaction (aza–ene reaction),[11] in which the C=C bond of enamine can be considered as a 2π system, the N-H of enamine as a 2σ system, and the ketone (Ph-C=O or Me-C=O) groups of diketone as 2π systems. Two types of reactions could be considered based on the ketone group used, with the first using the carbonyl of the benzoyl group (TS1a), and the second using the carbonyl of the acetyl group (TS1b). Each reaction has two possible steric approaches (*endo* and *exo*) depending on the positions of the alkyl and carbonyl groups not directly involved in the reaction.

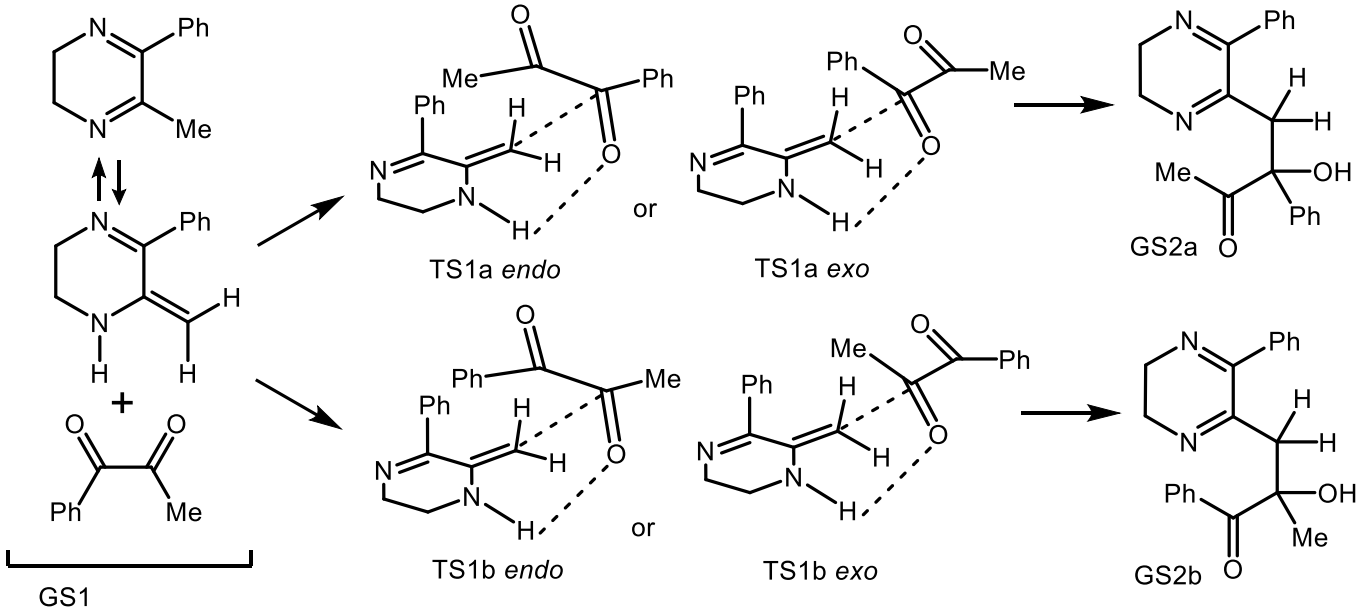

Figure 4. Proposed aldol reaction (aza–ene reaction) between 2-methylidene-3-phenyl-1,2,5,6-tetrahydropyrazine and 1-phenylpropane-1,2-dione

Each TS structure was then studied using saddle calculations *via* the semi-empirical PM7 molecular orbital calculation method,[12,13] and TS calculations were performed on the resulting structures at the B3LYP level of theory with the 6-31G(d) basis set. The obtained TS structures were then examined to

confirm which was the true TS using vibrational frequency analysis and intrinsic reaction coordinate calculations. The energy barrier, $\Delta E_{TS1\text{-}GS1}$ (kcal/mol), was the difference between the energy of the proposed TS1 and the energy of ground state 1 (GS1), given by the sum of the heats of formation of 2-methylidene-3-phenyl-1,2,5,6-tetrahydropyrazine and 1-phenylpropane-1,2-dione. Figure 5 shows the potential TS1 structures in the gas phase, with the C-C bonds to be formed and the proton transfer that must occur being marked along with their interatomic distances (Å).

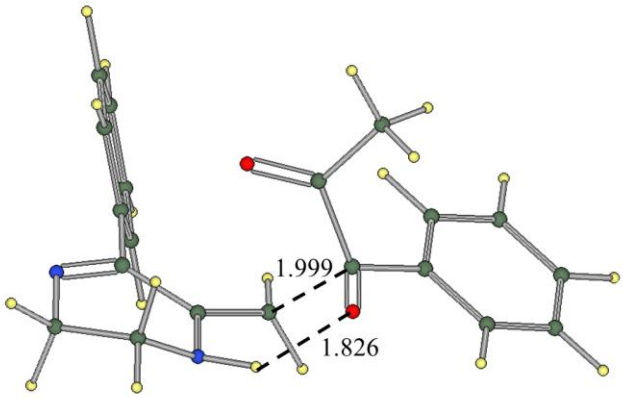

TS1a *endo* 13.98 kcal/mol

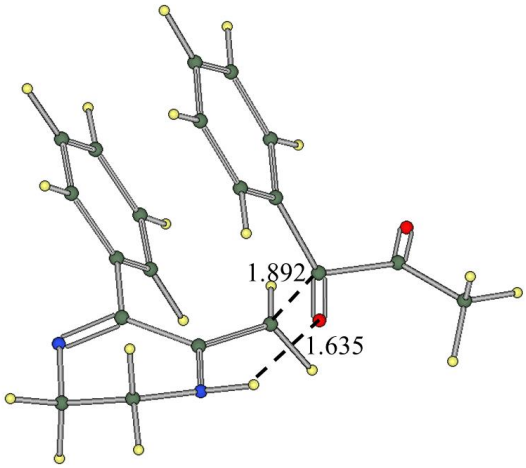

TS1a *exo* 14.88 kcal/mol

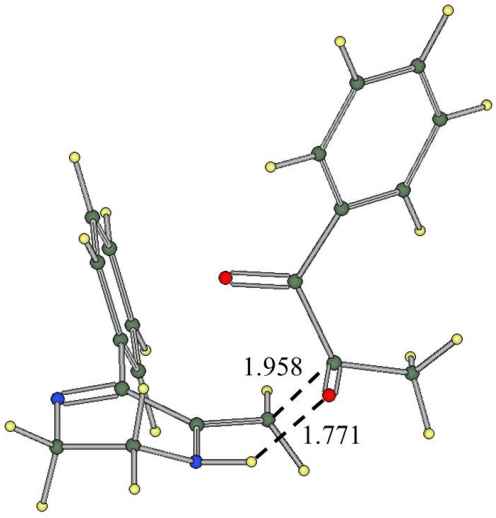

TS1b *endo* 19.39 kcal/mol

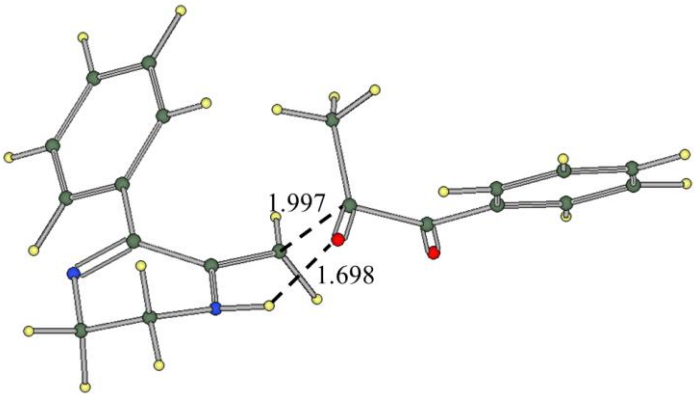

TS1b *exo* 16.12 kcal/mol

Figure 5. TS1 structures for possible aldol reaction, as calculated by the B3LYP/6-31(d) method

The dihedral angle of the diketone (∠O-C-C-O) in the TS1a *endo* structure was almost perpendicular (87.5°), while that of the TS1a *exo* structure was nearly flat (171.6°), similar to an *s*-*trans*-type diketone. The dihedral angles of the diketone (∠O-C-C-O) in TS1b *endo* and *exo* were 64.3° and 120.5°,

respectively. The TS1a *exo* structure, in which the benzene of 2-methylidene-3-phenyl-1,2,5,6-tetrahydropyrazine and the benzene of 1-phenylpropane-1,2-dione were parallel to each other, was relatively stable due to secondary orbital effects such as π–π interactions. TS1b *endo* was the least stable *endo* intermediate due to steric hindrance between the benzoyl group of 1-phenylpropane-1,2-dione and the benzene of 2-methylidene-3-phenyl-1,2,5,6-tetrahydropyrazine. The energy barriers in the gas phase showed that the reaction energy barrier was lower when using the carbonyl on the benzoyl group (TS1a *endo*) than when using the one on the acetyl group (TS1b *exo*) by approximately 2.1 kcal/mol, likely due to steric hindrance and secondary orbital effects that do not directly participate in the reaction. To investigate the impact of solvent effects on the reactivity, calculations incorporating MeOH and Et_2O as solvents were performed using the polarizable continuum model (PCM).[14] When the energy barriers considering MeOH and Et_2O were compared, the energy barrier when using the benzoyl group as the reaction site still tended to be lower than when using the acetyl group. Thus, it was found that this reaction tends to take place between the carbonyl of the benzoyl group (Ph-C=O) of diketone and enamine, which is a tautomer of the imine.

The suggested reaction mechanism is shown in Figure 6. 2,3-Dihydro-5-methyl-6-phenylpyrazine is in equilibrium with 2-methylidene-3-phenyl-1,2,5,6-tetrahydropyrazine, and so 2,3-dihydro-5-methyl-6-phenylpyrazine is first enaminated, then the aza–ene reaction occurs, followed by dehydration. Subsequent cyclization results in methyl rearrangement to form **product A**. As shown in Figure 6, **product B** can form *via* the reduction of GS3 *trans* using 2,3-dihydro-5-methyl-6-phenylpyrazine as a reducing agent, followed by cyclization *via* dehydration.[15,16]

In order to determine the structure of TS2 during the conversion of GS3 *cis* to **product A** *via* cyclization and rearrangement, the X-ray structure of **product A** was used as an initial set of coordinates to perform calculations at the B3LPY/6-31(d) level. Figure 7 shows the structure of TS2 for the intramolecular reaction of the imine and ketone. When the nitrogen lone pair of the imine approaches the carbon of the ketone, the methyl group of the ketone (Me-C=O) rearranges to the neighboring carbon. The energy barrier between the energies of TS2 and GS3 *cis*, $\Delta E_{\text{TS2-GS3}cis}$, was 22.71 kcal/mol in the gas phase. Using the PCM-B3LYP/6-31(d) method considering MeOH as the reaction solvent, the energy barrier was found to be 21.56 kcal/mol, 1.2 kcal/mol lower than in the gas phase, indicating that the reaction was more likely to proceed when using MeOH as a solvent.

In this study, we clarified the structures of the products yielded by the reaction of a cyclic 1,4-diazadiene and a diketone in MeOH as a solvent (**products A** and **B**) by 2D-NMR and single-crystal X-ray analysis. Theoretical calculations allowed us to propose that an aza–ene mechanism analogous to the aldol reaction occurred *via* the formation of an enamine in the highly polar solvent MeOH, followed by cyclization.

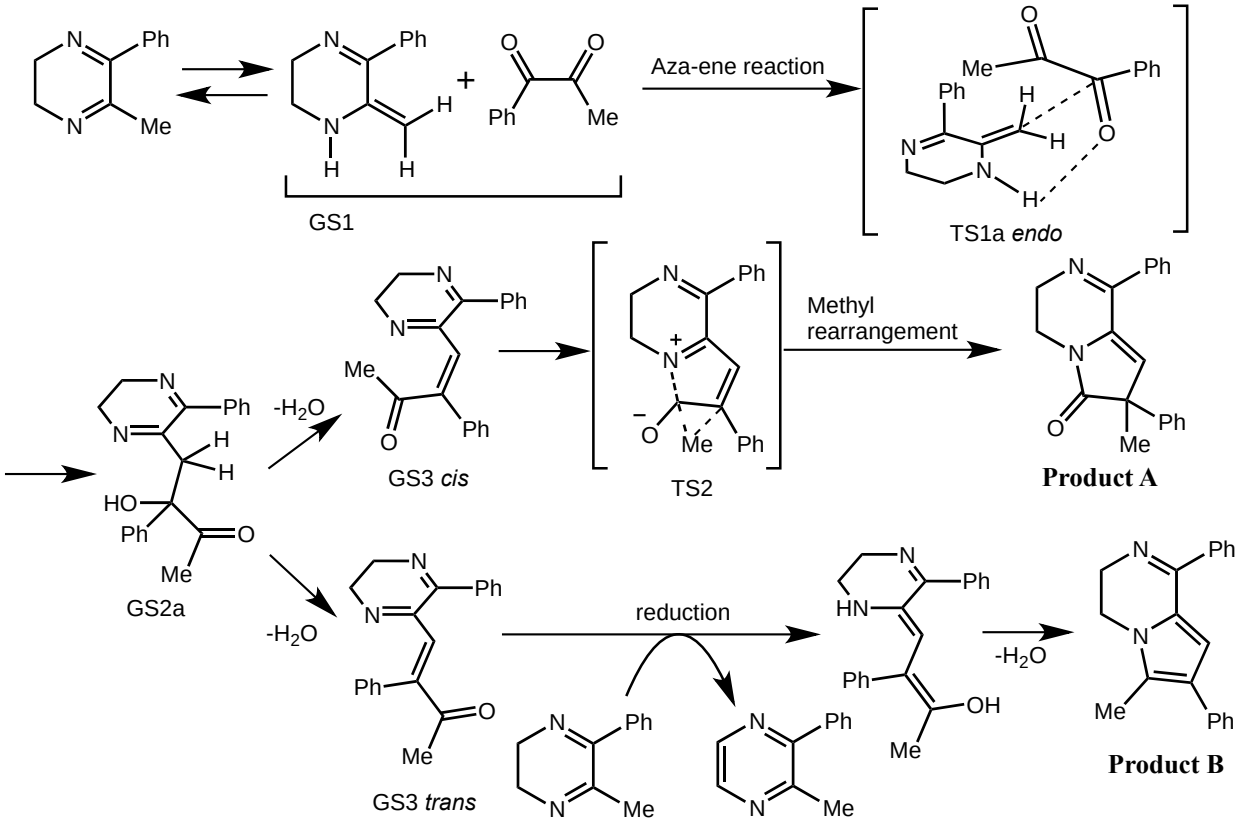

Figure 6. Proposed reaction mechanism

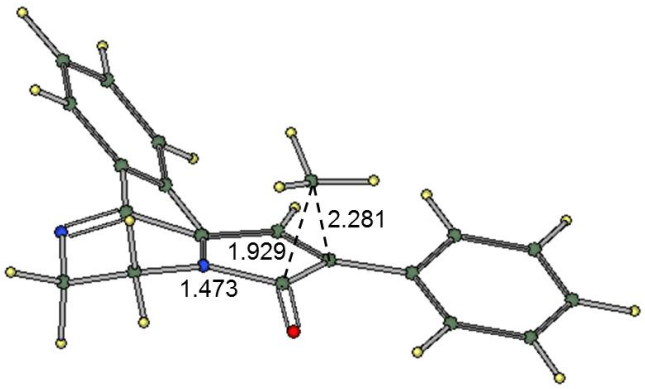

Figure 7. Structure of TS2 during the intramolecular reaction between the imine and ketone, as calculated using the B3LYP/6-31G(d) method

Structures with γ-lactam rings have been reported to inhibit platelet aggregation[17] and act as endothelium-cell dependent vasorelaxants,[18] and so **product A** can be expected to show biological activity; meanwhile, dihydropyrrolo[1,2-*a*]pyrazines such as those in **product B** have also been reported to show various bioactivities.[19] Currently, the details of the reaction mechanism such as the presence of the intermediates and the impact of solvent on reactivity are being investigated experimentally, with the formation of **product A** being monitored using HPLC. In the future, we will synthesize derivatives of these products and attempt to determine their biological activity.

EXPERIMENTAL

MATERIALS AND INSTRUMENTS

The reported melting points are uncorrected. IR spectra were obtained on a Hitachi 270-30 spectrophotometer. ^{1}H and ^{13}C NMR spectra were obtained on a JNM-ECA 500 (500 MHz) spectrometer using TMS (tetramethylsilane) as an internal standard. Mass spectra were obtained on a JMS-DX303HF instrument. Chemicals for the synthesis of 7-methyl-1,7-diphenyl-3,4-dihydropyrrolo[1,2-*a*]pyrazin-6(7*H*)-one and 6-methyl-1,7-diphenyl-3,4-dihydropyrrolo[1,2-*a*]pyrazine (**products A** and **B**) were purchased from Wako Pure Chemical Industries.

GENERAL EXPERIMENTAL PROCEDURE

The cyclic 1,4-diazadiene (**2,3-dihydro-5-methyl-6-phenylpyrazine**) was synthesized according to the literature.[20,21] A solution of ethylenediamine (0.25 g, 4 mmol) in Et_2O (4 mL) was added dropwise to a solution of 1-phenyl-1,2-propanedione (0.6 g, 4 mmol) in Et_2O (4 mL). After stirring at room temperature overnight, evaporation of the solvent gave the crude product, which was then frozen at −45 °C and purified by recrystallization from *n*-hexane.

Products A and **B** were synthesized *via* the reaction of a cyclic 1,4-diazadiene (2,3-dihydro-5-methyl-6-phenylpyrazine) and a diketone (1-phenyl-1,2-propanedione). A solution of ethylenediamine (0.25 g, 4 mmol) in MeOH (4 mL) was added dropwise to a solution of 1-phenyl-1,2-propanedione (0.6 g, 4 mmol) in MeOH. After dropwise addition, a small amount of H_2O was added to the reaction mixture to act as a catalyst. After stirring at room temperature overnight, the solvent was evaporated. The mixture was purified by chromatography on silica gel using a mixture of benzene and EtOAc as an eluent.

7-Methyl-1,7-diphenyl-3,4-dihydropyrrolo[1,2-*a*]pyrazin-6(7*H*)-one (**Product A):** colorless prisms. Yield 40.0%. mp 152–154 °C. IR (KBr) cm^{-1}: 1707.7 (C=O), 1447.3 (C=N). ^{1}H NMR (500 MHz, $CDCl_3$) δ: 1.72 (3H, s, CH_3), 3.66–3.70 (2H, m, CH_2), 4.07 (2H, s, CH_2), 5.93 (1H, s, CH), 7.28–7.73 (10H, m, aromatic-H). ^{13}C NMR (125 MHz, $CDCl_3$) δ: 23.7 (CH_3), 35.7 (CH_2), 49.2 (CH_2), 54.8 (C7), 111.7 (C9), 120.2 (C8), 126.4, 127.6, 128.2, 128.6, 128.9, 130.6, 131.0, 136.5, 139.5, 142.1 (aromatic-C), 160.0 (C=N), 178.7 (C=O). FAB-MS (*m/z*): 303.2 (M^++1). *Anal*. Calcd for $C_{20}H_{18}N_2O$: C, 79.44; H, 6.00; N, 9.26. Found: C, 79.17; H, 5.96; N, 9.14.

6-Methyl-1,7-diphenyl-3,4-dihydropyrrolo[1,2-*a*]pyrazine (**Product B):** yellowish crystals. Yield 19.8%. mp 186–188 °C. IR (KBr) cm^{-1}: 1476.2 (C=N). ^{1}H NMR (500 MHz, $CDCl_3$) δ: 2.40 (3H, s, CH_3), 3.92–3.93 (2H, m, CH_2), 4.03 (2H, s, CH_2), 6.52 (1H, s, CH), 6.91–7.79 (10H, m, aromatic-H). ^{13}C NMR (125 MHz, $CDCl_3$) δ: 10.6 (CH_3), 39.2 (C4), 47.9 (C3), 112.5 (C8), 123.3 (C7), 123.7 (C6), 125.9 (C9),

128.1, 128.3, 128.6, 128.8, 129.9, 136.1, 138.3 (aromatic-C), 160.5 (C=N). FAB-MS (*m/z*): 287.1 (M^++1). HR-MS Calcd for $C_{20}H_{19}N_2$ (M^++H): 287.1548. Found: 287.1528.

MOLECULAR ORBITAL (MO) CALCULATIONS

Semi-empirical MO calculations were performed through the Winmostar (GE) V4.105 interface[12] using MOPAC2016[13] on an Intel personal computer. Structures were optimized using semi-empirical methods and used as the starting geometries for the DFT calculations.[7] The energies were corrected using zero-point vibrational energy (scaled by a factor of 1.000). Calculations incorporating solvent effects in MeOH used the polarizable continuum model (PCM)[14] method included in the GAMESS software package. In the PCM method, the whole solvent is regarded as a continuum (reaction field) having a uniform relative dielectric constant ε, and a solute is set in a cavity therein: e.g., the dielectric constants of MeOH and Et_2O are 32.63 and 4.335, respectively. The data calculated on the B3LYP/6-31G(d) level are available upon request from the author.

SINGLE-CRYSTAL X-RAY ANALYSIS

A colorless prism crystal having approximate dimensions of 0.500 mm × 0.500 mm × 0.500 mm was mounted on a glass fiber. All measurements were made on a Rigaku RAXIS RAPID imaging plate area detector with graphite monochromatized Mo-Kα radiation. The data were collected at a temperature of 23±1 °C to a maximum 2θ value of 54.9°. The structures were solved by the direct method (SIR-2011),[22] and hydrogen atoms were placed as calculated. A full-matrix least-squares technique was used with anisotropic thermal parameters for non-hydrogen atoms and a riding model for hydrogen atoms. All the calculations were performed using the Crystal Structure[23,24] crystallographic software package. **Product A:** $C_{20}H_{18}N_2O_1$, monoclinic, space group *P1 21/n 1*, *a* = 5.5505(4), *b* = 10.4043(9), *c* = 27.401(2) (Å), β (°) = 91.707(2), *V* = 1581.7(2) ($Å^3$), Density (calc.) 1.270, Density (obs.) 1.271 g cm^{-3}, *Z* = 4, *R* = 0.0731, Unique data used = 3614, R_w = 0.2673, goodness of fit = 1.163. The crystallographic data are deposited at CCDC 1906158.

ACKNOWLEDGEMENTS

We thank Mr. K. Nakamura for experimental assistance.

REFERENCES AND NOTES

1. E. Vitaku, D. T. Smith, and J. T. Njardarson, *J. Med. Chem.*, 2014, **57**, 10257.
2. J. A. Maga and C. E. Sizer, *J. Agric. Food Chem.*, 1973, **21**, 22.
3. P. B. Miniyar, P. R. Murumkar, P. S. Patil, M. A. Barmade, and K. G. Bothara, *Mini-Rev. Med.*

Chem., 2013, **13**, 1607.

4. E. Lemp, A. L. Zanocco, G. Gunther, and N. Pizarro, *J. Org. Chem.*, 2003, **68**, 3009.
5. K. Nakahara, K. Yamaguchi, Y. Yoshitake, T. Yamaguchi, and K. Harano, *Chem. Pharm. Bull.*, 2009, **57**, 846.
6. D. Gopal, D. Macikenas, L. M. Sayre, and J. D. Protasiewicz, *Acta Chem. Scand.*, 1997, **51**, 938.
7. GAMESS, M. W. Schmidt, K. K. Baldridge, J. A. Boatz, S. T. Elbert, M. S. Gordon, J. J. Jensen, S. Koseki, N. Matsunaga, K. A. Nguyen, S. Su, T. L. Windus, M. Dupuis, and J. A. Montgomery, *J. Comput. Chem*., 1993, **14**, 1347.
8. G. A. Hill and E. W. Flosdorf, *Org. Synth.*, 1925, **5**, 91.
9. S. Ito, T. Hirano, A. Sugimoto, H. Kagechika, S. Takechi, and T. Yamaguchi, *Chem. Pharm. Bull*., 2010, **58**, 922.
10. H. Maruoka, N. Kashige, F. Miake, and T. Yamaguchi, *Chem. Pharm. Bull*., 2005, **53**, 1359.
11. S. Bahmanyar and K. N. Houk, *J. Am. Chem. Soc*., 2001, **123**, 11273.
12. Winmostar Version (GE) V4.105, X-Ability Co. Ltd., Tokyo, Japan, 2014.
13. MOPAC2016, J. J. P. Stewart, Stewart Computational Chemistry, Colorado Springs, Co, USA, http://OpenMOPAC.net, 2016.
14. J. Tomasi and M. Persico, *Chem. Rev.*, 1994, **94**, 2027.
15. S. J. Chen and F. W. Fowler, *J. Org. Chem*., 1971, **36**, 4025.
16. T. Shibamoto and R. A. Bernhard, *Agric. Biol. Chem*., 1977, **41**, 143.
17. H. Uchio, N. Shionozaki, Y. Kobayakawa, H. Nakagawa, and K. Makino, *Bioorg. Med. Chem. Lett.*, 2012, **22**, 4765.
18. C. Y. Kwan, P. H. M. Harison, P. A. Duspara, and E. E. Daniel, *Jpn. J. Pharmacol.*, 2001, **85**, 234.
19. A. Dagar, G. H. Bae, J. H. Lee, and I. Kim, *J. Org. Chem*., 2019, **84**, 6916.
20. T. Ishiguro and M. Matsumura, *Yakugaku Zasshi*, 1958, **78**, 229.
21. S. Ito, S. Takechi, K. Nakahara, N. Kashige, and T. Yamaguchi, *Chem. Pharm. Bull*., 2010, **58**, 825.
22. SIR2011: M. C. Burla, R. Caliandro, M. Camalli, B. Carrozzini, G. L. Cascarano, C. Giacovazzo, M. Mallamo, A. Mazzone, G. Polidori, and R. Spagna, *J. Appl. Cryst*., 2012, **45**, 357.
23. Crystal Structure 4.3: Crystal Structure Analysis Package, Rigaku Corporation (2000-2018). Tokyo 196-8666, Japan.
24. CRYSTALS Issue 11: J. R. Carruthers, J. S. Rollet, P. W. Betteridge, D. Kinna, L. Pearce, A. Larsen, and E. Gabe, Chemical Crystallography Laboratory, Oxford, U.K., 199 (Start here.)